

Phase-transition mechanism in $(\text{NH}_4)_2\text{SO}_4$

D. De Sousa Meneses, G. Hauret, and P. Simon

Centre de Recherche sur la Physique des Hautes Températures, C.N.R.S., 45071 Orleans Cedex 2, France

F. Bréhat and B. Wyncke

Laboratoire Infrarouge Lointain, Université Henri Poincaré, Nancy 1, BP 239, 54506 Vandoeuvre lès Nancy Cedex, France

(Received 8 September 1994)

The temperature dependence of the midinfrared reflectivity spectra of ammonium sulfate is reported for the two polarizations a and c of the electric field of the infrared wave, in the paraelectric and ferroelectric phases. Strong dynamic disorder of ammonium sulfate is confirmed by the occurrence in the paraelectric phase of vibration modes symmetry allowed only in the ferroelectric phase. Contrary to the molecular distortion-type-model predictions, no softening of the ν_3 or ν_4 (SO_4^{2-}) internal modes is observed. The comparison between low-frequency ($50\text{--}400\text{ cm}^{-1}$) reflectivity spectra of $(\text{NH}_4)_2\text{SO}_4$ and isomorphous crystals such as K_2SO_4 , mixed $(\text{K-NH}_4)_2\text{SO}_4$, and $(\text{Rb-NH}_4)_2\text{SO}_4$, shows that ammonium disorder induces sulfate disorder in the paraelectric phase. This underlines the important role of the librational B_{1u} sulfate mode in the phase-transition mechanism. The microscopic origin of the critical relaxation is assigned to reorientation of the whole group $\text{NH}_4^+(\text{I})\text{-(SO}_4^{2-})\text{-NH}_4^+(\text{II})$ between two equivalent positions with regard to the ab mirror plane. The behavior of the spontaneous polarization is well explained by two contributions, a lattice part and a part due to distortion of all the ions. Finally a softeninglike behavior of the ν_3 (NH_4^+) mode is observed and explained in the light of hard-mode spectroscopy.

I. INTRODUCTION

Ammonium sulfate $[(\text{NH}_4)_2\text{SO}_4]$, hereafter denoted AS) undergoes a first-order ferroelectric phase transition at 223 K .¹⁻³ Peculiar ferroelectric properties of this compound are the small value (about 15 K) of the Curie-Weiss constant⁴ and especially the temperature dependence of the spontaneous polarization, which vanishes and changes sign 138 K below T_C .^{5,6} The phase-transition mechanism inducing these properties is not yet well understood, despite many investigations. In both phases, the unit cell contains four formula units with two nonequivalent ammonium ions $\text{NH}_4^+(\text{I})$ and $\text{NH}_4^+(\text{II})$ and one kind of SO_4^{2-} .⁷ The change of space group from $Pnam(D_{2h}^{16})$ to $Pna2_1(C_{2v}^9)$ characterized by the loss of mirror plane ab and of the center of inversion allows the appearance of spontaneous polarization along the c axis. The ferroelectric distortion transforms as the B_{1u} representation in the paraelectric phase which correlates with the A_1 representation in the ferroelectric phase.

The dynamics of the phase transition is somewhat complex. Recently, an infrared investigation of the dielectric dispersion in the $4\text{--}400\text{ cm}^{-1}$ range has confirmed the critical slowing down of a soft dielectric relaxation of B_{1u} symmetry.⁸ Its relaxation time τ_s fulfills the classical law $\tau_s^{-1} = \gamma(T - T_0)$ with the same parameters as those determined previously in the GHz range.⁹ Some authors suggest that the origin of this relaxation is connected with the disorder of both ammonium ions and more probably to a reorientation of NH_4^+ groups about the a axis at an angle $\pm 20^\circ\text{--}30^\circ$ from the (001) plane.^{8,10,11}

Besides this low-frequency critical relaxation, noncritical broad absorption was observed in the submillimeter range for all polarizations. This dispersion was described by relaxations of frequencies about $20\text{--}60\text{ cm}^{-1}$, assigned by Kozlov *et al.*⁸ to anharmonic librations of SO_4^{2-} . On the other hand, critical x-ray diffuse scattering was reported by Hasebe and Tanisaki^{12,13} According to them, the diffuse-scattering intensity distribution cannot be explained by the other-disorder behavior of ammonium ions, but can originate from the librational B_{1u} mode of sulfate ions. Moreover, the spontaneous displacement of the sulfate ions at the transition corresponds to the condensation of the librational mode at the phase transition from the paraelectric phase.

Other instabilities have been evidenced in light scattering spectra. Two of them occur in the totally symmetric A_g Raman spectra: the vanishing below T_C of the broad central components and the strong discontinuity of a mode at about 40 cm^{-1} .^{8,14-17} These low-frequency peaks are attributed to reorientations of both NH_4^+ and SO_4^{2-} groups. Anomalies were also observed in Brillouin spectra: from measurements above T_C in pure AS and mixed $(\text{Rb-NH}_4)_2\text{SO}_4$, Unruh *et al.*¹⁵ explain the temperature anomaly of the elastic constant C_{11} by a linear coupling of strain with the A_g central component. Both A_g and B_{1u} symmetries might become relevant at the transition because partial substitution of NH_4^+ groups by Rb atoms reduces the A_g instability with regard to the B_{1u} instability. Moreover, as the Rb atoms substitute preferentially for $\text{NH}_4^+(\text{II})$ groups, Kozlov *et al.*⁸ argued that B_{1u} ordering, which represents the primary order parameter, consists essentially of $\text{NH}_4^+(\text{I})$ ordering whereas

$\text{NH}_4^+(\text{II})$ are more involved in A_g ordering. A_g ordering then represents a secondary order parameter, triggered by the first one.

In addition to these modifications, both B_{1u} and A_g distortions appear below T_C , including a large spontaneous strain¹⁸ and internal distortions of all the ions.^{19,20} Spontaneous strain and distortion of SO_4^{2-} ions display a large increase at T_C with minor temperature dependence below T_C . The NH_4^+ ions distort even more, but more gradually below T_C .^{13,19} In the light of the behavior of SO_4^{2-} , Jain and co-workers^{19,20} suggest that the phase transition is of molecular distortion type and the internal sulfate ν_3 mode should be the favored mode triggering the transition.

Some investigations of the dynamical reorientation of ammonium ions have been performed,^{10,21–24} but there are discrepancies concerning the magnitude of the relaxation rates.⁸ However, one can describe the typical behavior of reorientation of ammonium groups. According to Goyal *et al.*,²⁴ the reorientational motions do not change significantly over the paraelectric-to-ferroelectric phase transition and are nearly of the same magnitude for both ions. The dynamical distinction between the two ions occurs in the ferroelectric phase and the temperatures of ordering seen by NMR are respectively ~ 165 and ~ 120 K for $\text{NH}_4^+(\text{I})$ and $\text{NH}_4^+(\text{II})$.^{10,21} These temperatures are in good agreement with the appearance of the NH_4^+ harmonic librational modes at about 365 and 395 cm^{-1} in Raman scattering.¹⁴

In the light of the previous results and the fact that crystals such as K_2SO_4 or Rb_2SO_4 present neither ferroelectric phase transition nor disorder, it is clear that disorder plays an important part in the mechanism of the phase transition in AS. To discuss more precisely the influence of disorder on AS groups and probe the behavior of ν_3 stretching SO_4^{2-} modes, we decided to perform infrared reflectivity experiments in the spectral range of internal SO_4^{2-} and NH_4^+ modes (400–4000 cm^{-1}) as quoted by Kozlov *et al.*⁸ Infrared reflectivity is a powerful tool to investigate any ferroelectric instability on both sides of T_C , as any softlike ferroelectric mode will be ir active. (Kwun *et al.*²⁵ have reported reflectivity data at some temperatures below T_C , but the knowledge of sulfate ν_3 -mode behavior at the phase transition is still unknown, and the analysis of experimental data was car-

ried out only by Kramers-Krönig inversion.) A comparison of low-frequency (50–400 cm^{-1}) spectra between $(\text{NH}_4)_2\text{SO}_4$, K_2SO_4 , and mixed $(\text{K-NH}_4)_2\text{SO}_4$ and $(\text{Rb-NH}_4)_2\text{SO}_4$ (hereafter K-As and Rb-As) is also done to underline the crucial role of the B_{1u} librational sulfate mode. Finally, an explanation of the peculiar polarization behavior of AS is proposed and discussed in the light of infrared hard-mode spectroscopy.²⁶

II. EXPERIMENTAL PROCEDURE

Single crystals of $(\text{NH}_4)_2\text{SO}_4$ were grown from saturated aqueous solutions by slow evaporation. The sample used in the present study was a platelet about $15 \times 15 \times 2$ mm^3 in size. The infrared reflectivity spectra have been recorded on a coupled Bruker IFS113v-IFS88 rapid-scan Fourier transform interferometer, giving access to the spectral range 10–40 000 cm^{-1} . Low temperatures were obtained by using a liquid-helium cryostat, with KRS-5 (thallium bromide, near infrared) windows. The temperature stability is better than 0.1 K.

III. ANALYSIS OF INFRARED REFLECTIVITY SPECTRA

A. Dielectric-function models

Infrared reflection spectroscopy provides, via Fresnel's relation near normal incidence, the complex dielectric function ϵ

$$R = \left| \frac{\sqrt{\epsilon} - 1}{\sqrt{\epsilon} + 1} \right|^2, \quad (1)$$

where R is the reflectance. Theoretically it is possible to deduce the real and imaginary parts of the dielectric function through a Kramers-Krönig analysis of the reflection data, but this often leads to some uncertainties or mistakes due to the extension to zero and infinity of the low- and high-frequency edges of the experimental data, particularly when these edges are not flat. Another way is to use a model of the dielectric function, and to fit its adjustable parameters to the experimental reflection spectra through Fresnel's relation.

The factorized form, or four-parameter model,

TABLE I. Reduction into irreducible representations of the 108 internal modes of $(\text{NH}_4)_2\text{SO}_4$ in the paraelectric phase. The tetrahedron internal modes, are indicated with Herzberg's notation.

	$\text{NH}_4^+(\text{I})$	Internal modes $\text{NH}_4^+(\text{II})$	SO_4^{2-}	Basis function	Raman and ir activities
A_g	$\nu_1 + \nu_2 + 2\nu_3 + 2\nu_4$	$\nu_1 + \nu_2 + 2\nu_3 + 2\nu_4$	$\nu_1 + \nu_2 + 2\nu_3 + 2\nu_4$	xx, yy, zz	Raman
B_{1g}	$\nu_1 + \nu_2 + 2\nu_3 + 2\nu_4$	$\nu_1 + \nu_2 + 2\nu_3 + 2\nu_4$	$\nu_1 + \nu_2 + 2\nu_3 + 2\nu_4$	xy	Raman
B_{2g}	$\nu_2 + \nu_3 + \nu_4$	$\nu_2 + \nu_3 + \nu_4$	$\nu_2 + \nu_3 + \nu_4$	xz	Raman
B_{3g}	$\nu_2 + \nu_3 + \nu_4$	$\nu_2 + \nu_3 + \nu_4$	$\nu_2 + \nu_3 + \nu_4$	yz	Raman
A_u	$\nu_2 + \nu_3 + \nu_4$	$\nu_2 + \nu_3 + \nu_4$	$\nu_2 + \nu_3 + \nu_4$		
B_{1u}	$\nu_2 + \nu_3 + \nu_4$	$\nu_2 + \nu_3 + \nu_4$	$\nu_2 + \nu_3 + \nu_4$	z	ir
B_{2u}	$\nu_1 + \nu_2 + 2\nu_3 + 2\nu_4$	$\nu_1 + \nu_2 + 2\nu_3 + 2\nu_4$	$\nu_1 + \nu_1 + 2\nu_3 + 2\nu_4$	y	ir
B_{3u}	$\nu_1 + \nu_2 + 2\nu_3 + 2\nu_4$	$\nu_1 + \nu_2 + 2\nu_3 + 2\nu_4$	$\nu_1 + \nu_2 + 2\nu_3 + 2\nu_4$	x	ir

TABLE II. As in Table I, but in the ferroelectric phase.

	$\text{NH}_4^+(\text{I})$	Internal modes $\text{NH}_4^+(\text{II})$	SO_4^{2-}	Basis function	Raman and ir activities
A_1	$\nu_1+2\nu_2+3\nu_3+3\nu_4$	$\nu_1+2\nu_2+3\nu_3+3\nu_4$	$\nu_1+2\nu_2+3\nu_3+3\nu_4$	xx,yy,zz,z	Raman, ir
A_2	$\nu_1+2\nu_2+3\nu_3+3\nu_4$	$\nu_1+2\nu_2+3\nu_3+3\nu_4$	$\nu_1+2\nu_2+3\nu_3+3\nu_4$	xy	Raman
B_1	$\nu_1+2\nu_2+3\nu_3+3\nu_4$	$\nu_1+2\nu_2+3\nu_3+3\nu_4$	$\nu_1+2\nu_2+3\nu_3+3\nu_4$	xz,x	Raman, ir
B_2	$\nu_1+2\nu_2+3\nu_3+3\nu_4$	$\nu_1+2\nu_2+3\nu_3+3\nu_4$	$\nu_1+2\nu_2+3\nu_3+3\nu_4$	yz,y	Raman, ir

$$\epsilon(\omega) = \epsilon_\infty \prod_j \frac{\Omega_{j\text{LO}}^2 - \omega^2 + i\omega\gamma_{j\text{LO}}}{\Omega_{j\text{TO}}^2 - \omega^2 + i\omega\gamma_{j\text{TO}}}, \quad (2)$$

was proposed by Kurosawa²⁷ and works well in numerous cases, including strongly damped soft modes.²⁸ In this model, each optical model [transverse (TO) or longitudinal (LO)] is described by two parameters, frequency Ω_j and damping γ_j . The TO modes are the complex poles of ϵ while the LO modes are the complex zeros. Thus the imaginary part of ϵ represents the structure of TO modes while the structure of LO modes is given by the imaginary part of $1/\epsilon$. This model is an extension to finite frequencies of the Lyddane-Sachs-Teller relation. From the whole set of TO and LO frequencies, one can calculate the dielectric strength of each mode (often also called the oscillator strength)

$$\Delta\epsilon_j = \epsilon_\infty \Omega_{j\text{TO}}^{-2} \frac{\prod_k (\Omega_{k\text{LO}}^2 - \Omega_{j\text{TO}}^2)}{\prod_{k \neq j} (\Omega_{k\text{TO}}^2 - \Omega_{j\text{TO}}^2)}, \quad (3)$$

and the static dielectric constant (assuming there is no dispersion below the infrared spectral range)

$$\epsilon(\omega=0) = \epsilon_\infty + \sum_j \Delta\epsilon_j. \quad (4)$$

B. Symmetry of the internal modes

In both paraelectric and ferroelectric phases, $(\text{NH}_4)_2\text{SO}_4$ contains four formula units per primitive cell, leading to 108 internal modes. Tables I (paraelectric) and II (ferroelectric) show how the internal modes transform as the irreducible representations of the space groups. This classification assumes local symmetry $m(C_s)$ for all tetrahedra, viz., averaged positions, in the paraelectric phase, and $1(C_1)$ symmetry in the ferroelectric phase.

IV. RESULTS

The experimental spectra were obtained from liquid nitrogen up to room temperature for the two polarizations a and c of the electric field of the electromagnetic ir wave, corresponding to B_{3u} and B_{1u} irreducible representations above T_C , and to B_1 and A_1 below T_C . As one can see in Figs. 1 and 2, in the ferroelectric phase, although the sample shatters at T_C , this does not alter the quality of the infrared reflectivity spectra. However, in the

2500–3500 cm^{-1} range, the magnitude of the reflectivity is underestimated because of diffusion at the sample surface. But this systematic error does not preclude the interpretation of the qualitative variation of the internal modes.

All spectra were simulated with the four-parameter model. From the resulting set of frequencies and dampings, one obtains the TO-mode structures which are given by the imaginary part of the dielectric function (Figs. 3 and 4). Mode assignment is indicated in these figures. In both polarizations, the internal modes of SO_4^{2-} lie in the 400–1200 cm^{-1} spectral range while those of NH_4^+ groups are situated above 1300 cm^{-1} . In symmetries A_1 and B_1 , 10 and 13 oscillators were respectively used for the fit of the reflectivity spectra in the ferroelectric phase while seven oscillators were used in the paraelectric phase for both symmetries. A discrepancy appears between the number of oscillators predicted by group theory and that obtained by simulation. In the paraelectric phase, some

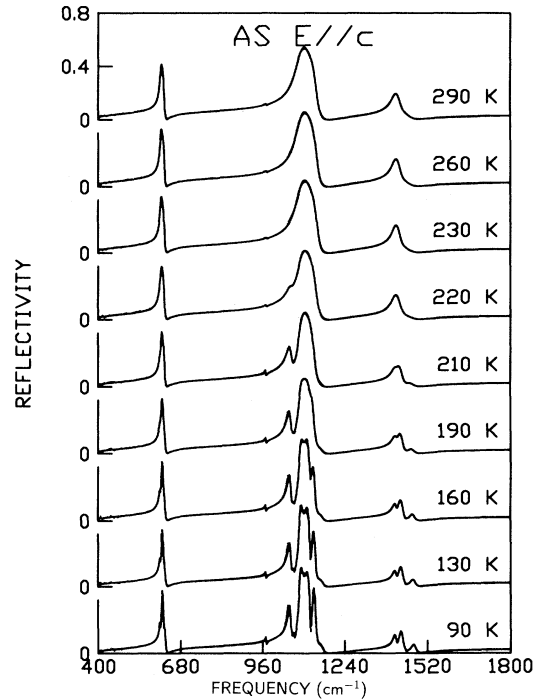


FIG. 1. Temperature dependence of the infrared reflectivity spectra of AS for polarization of the ir wave along the c axis (B_{1u} symmetry). Dots: experiment; full lines: best fit performed with the factorized form of the dielectric function.

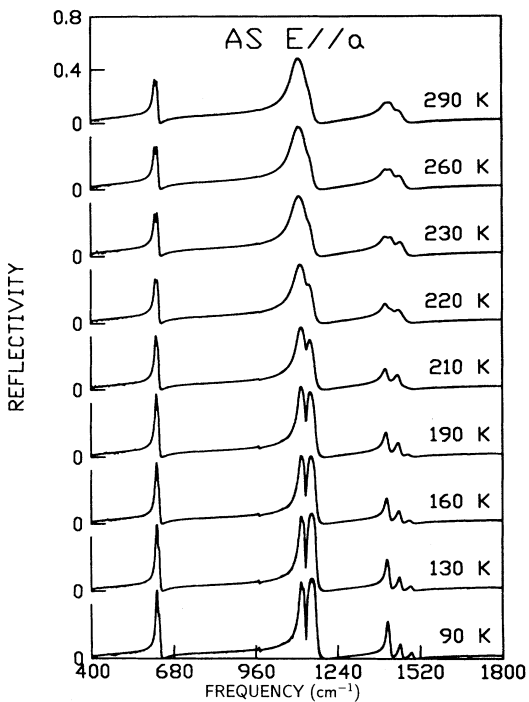


FIG. 2. Temperature dependence of the infrared reflectivity spectra of AS for polarization of the ir wave along the a axis (B_{3u} symmetry). Dots: experiment; full lines: best fit performed with the factorized form of the dielectric function.

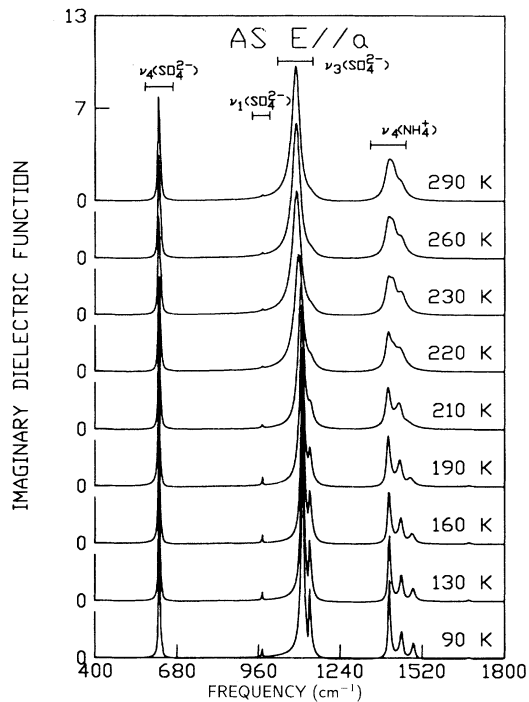


FIG. 4. Imaginary dielectric function (TO-mode structure) for polarization of the ir wave along the a axis, obtained by the best fit of the factorized form of ϵ .

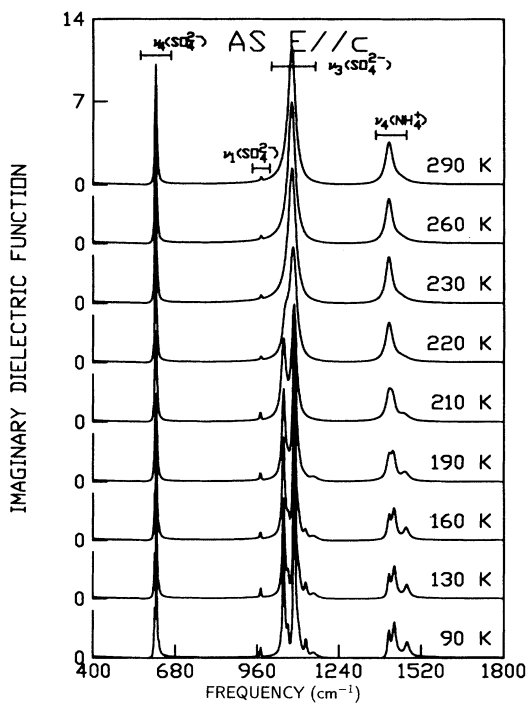


FIG. 3. Imaginary dielectric function (TO-mode structure) for polarization of the ir wave along the ferroelectric c axis, obtained by the best fit of the factorized form of ϵ .

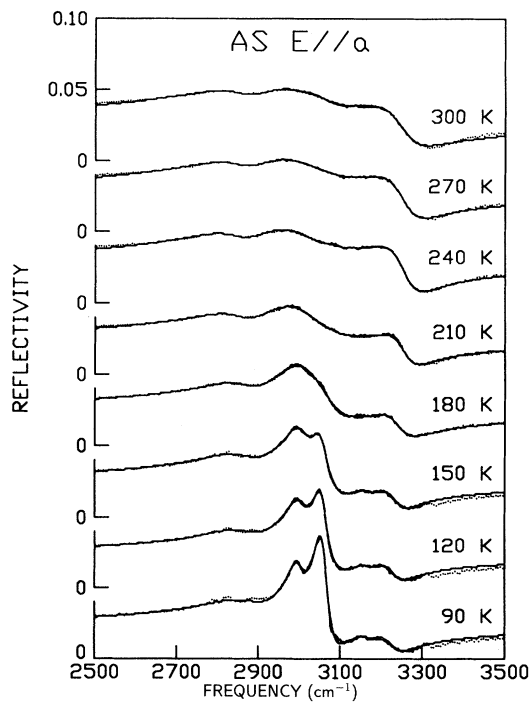


FIG. 5. Temperature dependence of the high-frequency infrared reflectivity spectra of AS for polarization of the ir wave along the a axis (B_{3u} symmetry). Dots: experiment; full lines: best fit performed with the factorized form of the dielectric function.

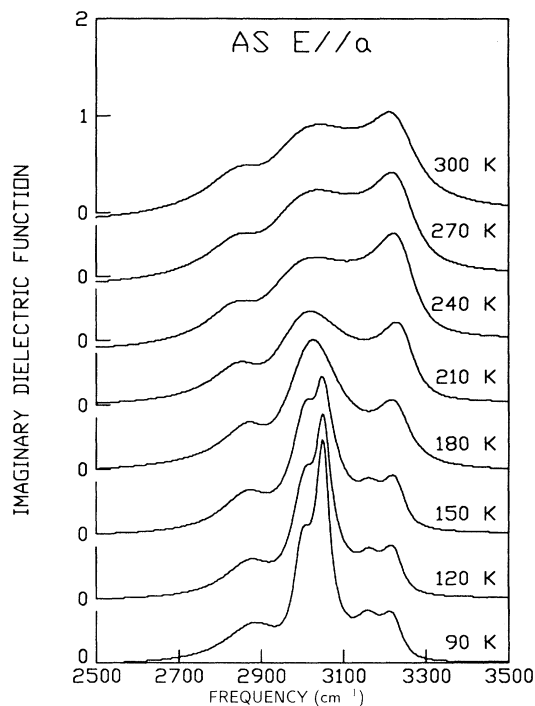


FIG. 6. Imaginary dielectric function (TO-mode structure) at high frequency for polarization of the ir wave along the a axis, obtained by the best fit of the factorized form of ϵ .

modes symmetry allowed only in the ferroelectric phase are nevertheless present. In B_{1u} symmetry, there are three supplementary forbidden internal modes: ν_1 , $\nu_4(\text{SO}_4^{2-})$ and $\nu_4(\text{NH}_4^+)$ while in B_{3u} symmetry, one $\nu_4(\text{NH}_4^+)$ supplementary mode occurs. In the ferroelectric phase, the simulation agrees with group theory apart from $\nu_3(\text{SO}_4^{2-}) A_1$ modes, for which three weak supplementary oscillators become visible. Most of the additional modes appear at the transition, but it looks as if the apparition of the new NH_4^+ modes is more progressive than that of SO_4^{2-} . Besides, there is no distinction between $\nu_4[\text{NH}_4^+(\text{I})]$ and $\nu_4[\text{NH}_4^+(\text{II})]$ modes. Furthermore, a $\nu_3(\text{SO}_4^{2-})$ mode becomes visible below 190 K in A_1 symmetry.

Figures 5 and 6 display high-frequency ammonium modes. The reflectivity spectra were fitted with three oscillators above 180 K and five below. Softeninglike behavior of a $\nu_3(\text{NH}_4^+)$ mode arises at about 10 K above the transition and a discrimination between the two kinds of ammonium appears below ~ 180 K.

V. DISCUSSION

A. The phase transition

In order to underline the main aspects of the phase transition, it is interesting to compare AS properties with those of compounds such as K_2SO_4 or Rb_2SO_4 . At room temperature, potassium and rubidium sulfates are iso-

morphous to AS, but upon cooling neither K_2SO_4 nor Rb_2SO_4 undergoes a ferroelectric phase transition. Hence, the substitution of isotropic ions by a tetrahedral NH_4^+ ion drastically modifies the structural and dynamic behavior. As alkaline sulfates present neither signatures of relaxation in the far-infrared range nor any sign of disorder in external modes (Fig. 7), disorder in AS is clearly involved in the phase-transition mechanism.

The occurrence of strong disorder in AS is obvious: besides the manifestations cited in the Introduction, the presence of several internal modes normally forbidden by symmetry such as the sulfate ν_1 mode in $E||c$ polarization is direct evidence of such disorder. Such an effect was already reported in other order-disorder transitions, as in sodium nitrite,²⁹ where the lattice modes characteristic of the low-temperature phase are always observable more than 50 K above T_C . The disorder in AS concerns not only NH_4^+ ions but also SO_4^{2-} ions: Hasebe¹³ has shown that above T_C the sulfate groups perform thermal librational motions with amplitude as large as $\pm 7^\circ$. This value looks to be too high for harmonic librations.¹³ Such an assertion is confirmed in the present study by the librational $\text{SO}_4^{2-} B_{1u}$ mode which is present at about 80 cm^{-1} in K_2SO_4 , with stronger damping in K-AS and Rb-AS, but is not visible in AS (Fig. 7). The absence of this librational mode in AS, certainly due to a too strong damping value, is direct evidence that ammonium disorder induces sulfate disorder in the paraelectric phase, and also a signature that this mode, particularly sensitive to

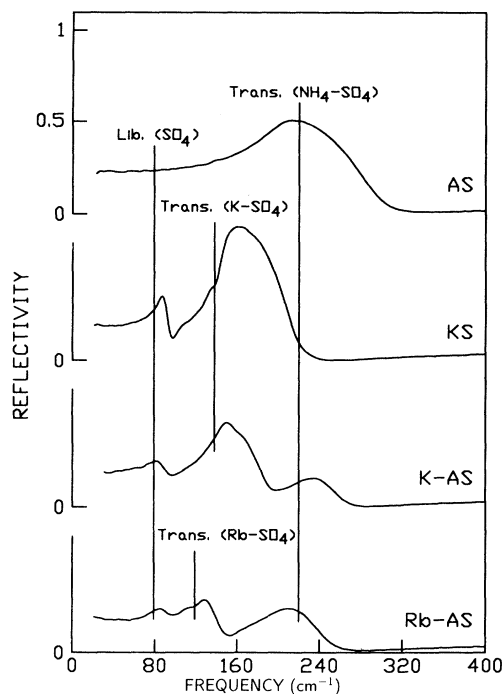


FIG. 7. Infrared reflectivity spectra of AS, KS (K_2SO_4), K-AS ($[\text{K}_{0.85}(\text{NH}_4)_{0.15}]_2\text{SO}_4$), and Rb-AS ($[\text{Rb}_{0.8}(\text{NH}_4)_{0.2}]_2\text{SO}_4$) at room temperature. The mode assignments are indicated on the spectra (polarization along the c axis, i.e., B_{1u} symmetry).

ammonium disorder, can play an important role at the phase transition.

Let us now discuss the behavior of sulfate and ammonium ions upon undergoing the phase transition. All the features due unambiguously to sulfate ions are discontinuous: (i) distortion of the tetrahedron,¹⁹ (ii) disappearance of Raman central components and strong discontinuity of a mode at about 40 cm^{-1} below T_C ,^{14,16} (iii) appearance of librational modes in the reflectivity spectra,³⁰ and (iv) splitting of the ν_3 mode in the ferroelectric phase. In contrast, anomalies attributed to ammonium ions (distortion of the tetrahedron¹⁹ or change of reorientation time²⁴) are more progressive. It follows that the first-order character of the phase transition mainly originates from sulfate groups as previously mentioned by Bajpai and Jain.²⁰

However, the present results show that there is no softening of ν_3 or ν_4 (SO_4^{2-}) internal modes. This does not support Bajpai's hypothesis in which the ν_3 (SO_4^{2-}) mode constitutes the main part of the order parameter, and thus the model of molecular distortion type is ruled out. Comparison of the sulfate ν_3 linewidths in the paraelectric and the ferroelectric phases does not show any broadening throughout T_C , and no noticeable change, apart from normal thermal effects, is observed between liquid-nitrogen and room temperatures. Moreover, as previously mentioned, most of the modifications associated with sulfate are sudden and it seems that sulfate groups become ordered just below T_C , as seen by the appearance of harmonic librations and vanishing of Raman central components.¹⁴ All this is in contradiction with the attribution of the noncritical submillimeter relaxation by Kozlov *et al.*⁸ to disorder of oxygen ions of sulfate groups. The relaxation time of this component does not reveal any critical anomaly near T_C . The relaxation strength, i.e., the contribution of the relaxation to $\epsilon(\omega=0)$, continuously decreases upon cooling and completely disappears below about 100 K. Such behavior is more compatible with reorientation of ammonium groups, which disappears below 120 K and does not present any sudden anomaly of relaxation time at T_C .^{14,24}

Concerning the slowing down of the critical B_{1u} relaxation, it is now well established that it constitutes the trigger of the phase transition. But this relaxation, if entirely assigned to ammonium and, more precisely, to hindered rotation of NH_4^+ about the a axis, cannot explain all the experimental results. Indeed, according to Hasebe,¹³ ammonium disorder cannot explain the critical x-ray diffuse scattering, whereas the condensation of the librational B_{1u} sulfate mode can explain not only this but also the displacement of sulfate groups at T_C .^{12,13} Then both sulfate and ammonium groups are involved in the mechanism of the critical relaxation. More precisely, this leads one to assume that the microscopic origin of this relaxation is the reorientation of the group $\text{NH}_4^+(\text{I})$ - (SO_4^{2-}) - $\text{NH}_4^+(\text{II})$ between two equivalent positions with regard to the ab mirror plane, as displayed in Fig. 8. This hypothesis is consistent with (i) the high anharmonicity of the librational B_{1u} sulfate mode in the paraelectric phase, (ii) the noncritical slowing down of the relaxation

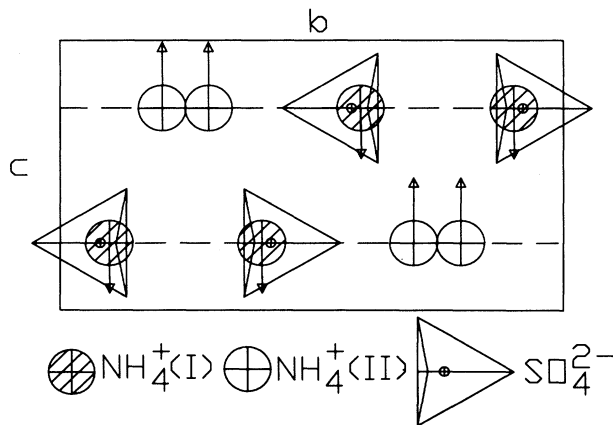


FIG. 8. Schematic projection of the ammonium sulfate structure onto the bc plane at $T=233\text{ K}$ based on the x-ray diffraction data of Hasebe (Ref. 13). The ammonium positions are the averaged values between their two sites. The arrows show the departure from the mirror plane of the averaged position of ammonium ions in the ferroelectric phase.

then assigned to reorientation of ammonium groups, (iii) all ionic displacements along the c axes, and (iv) the fact that the deviations from the ab mirror plane of the averaged positions of ammonium ions are proportional to the rotation angle of the sulfate.¹³

Another question about the nature of the phase transition is the origin of the anomalies in the A_g symmetry. Is it necessary to assume a secondary order parameter to explain A_g features as suggested by several authors,^{8,15} or is a coupling with the B_{1u} order parameter sufficient to account for this?

From Brillouin light scattering measurements above T_C on AS and on mixed Rb-AS, Unruh *et al.*¹⁵ explain the temperature dependence of the C_{11} elastic moduli by a linear coupling with the A_g central component. Moreover, due to the fact that partial substitution of NH_4^+ groups by Rb^+ ions reduces the A_g instability with regard to B_{1u} instability, they conclude that both A_g and B_{1u} symmetries might become active in the transition mechanism. However, upon reexamining the temperature dependence of C_{11} above and below T_C measured by Unruh *et al.*¹⁶ it appears that the linear coupling invoked to account for the anomalous part of the elastic constant cannot explain the large step observed at the transition for C_{11} . This step and the anomalous dependence part are characteristic of a coupling $\sim eQ^2$ linear in the strain e and quadratic in the order parameter Q . Hence an order parameter of B_{1u} symmetry which also satisfies the selection rules can explain this anomaly more satisfactorily.

Concerning the A_g Raman anomalies, viz., the sudden disappearance of the central components and the specific behavior of the 40 cm^{-1} mode at T_C ,¹⁶ we tentatively assign the central components to anharmonic librations of the sulfate ions and ammonium disorder as previously mentioned.¹⁴ The 40 cm^{-1} mode is attributed to the

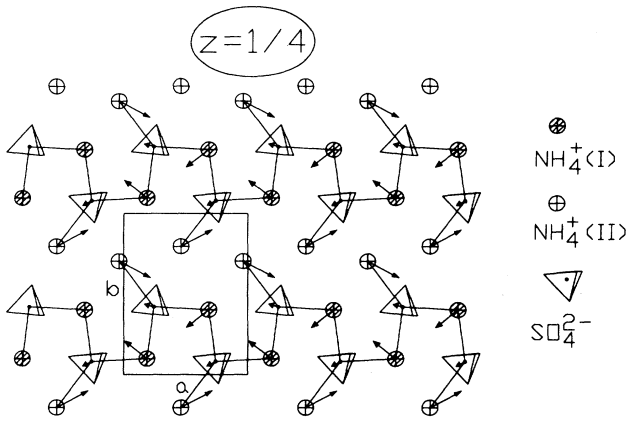


FIG. 9. Schematic projection of the ions lying in the ab mirror plane at $Z = \frac{1}{4}$ in the paraelectric phase. The displacements in the ab plane of the ions below T_C are represented by arrows.

pseudorotational motion sketched in Fig. 9, which corresponds to all the displacements of the ions in the ab plane at T_C . An explanation of this mode behavior can be made in the framework of hard-mode spectroscopy.^{8,26,31} The sudden change at the phase transition is possibly due to a linear coupling $Q_i Q_j$ between the normal coordinate Q_i of the 40 cm^{-1} hard mode and the B_{1u} order parameter Q_j . This assumption is consistent with the temperature dependence of the hard-mode frequency which undergoes a shift (8 cm^{-1}) at T_C and evolves linearly with the order parameter in the vicinity of the phase-transition temperature.¹⁶ Besides, the vanishing of the central peak is accompanied by the change into a Lorentzian line of the librational sulfate mode at $\sim 70 \text{ cm}^{-1}$. This agrees with attribution of the central peak to anharmonic librations of the sulfate ions.

Finally, let us deal with the dynamical behavior of the ammonium groups. Our investigation of the stretching ν_3 (NH_4^+) modes is in good agreement with the results of Raman scattering,¹⁴ NMR,²¹ and neutron scattering.²⁴ Indeed, the change of behavior between $\text{NH}_4^+(\text{I})$ and $\text{NH}_4^+(\text{II})$ is only visible below 180 K and is evidenced by the discrimination of ν_3 modes of both kinds of ammonium.

B. An explanation of the temperature dependence of the polarization

Two types of models of the microscopic origin of AS polarization have been proposed: the point-charge model³² and the ferroelectric-ordering models involving non-equivalent $\text{NH}_4^+(\text{I})$ and $\text{NH}_4^+(\text{II})$ ions of two crystallographically different sublattices.^{4,33-35} None of them is entirely satisfactory.¹⁷

On the basis of the x-ray diffraction data of Hasebe,¹³ the temperature dependence of the displacive lattice polarization can be calculated. As displayed in Fig. 8, the displacements below T_C from the ab mirror plane of the two kinds of ammonium are not identical. This difference is at the origin of the so-called lattice polariza-

tion, which has been neglected in previous models. As both kinds of ammonium ion behave as statistical elements, their average positions can be calculated by the following relation:

$$\Delta z_i = \Delta z_1^i P_1^i + \Delta z_2^i P_2^i, \quad (5)$$

where Δz_i , Δz_j^i , and P_j^i denote, respectively, the average deviation from the ab mirror plane of ammonium i , the position of the site j with regard to the ab mirror plane, and the occupation probability of the site j . Assuming the same point charge $+e$ for both kinds of ammonium and $-2e$ for the sulfate ion, we obtain the lattice polarization

$$P = 4 \times 10^2 \frac{e(|\Delta z_2| - |\Delta z_1|)}{abc}, \quad (6)$$

where a, b, c denote lattice parameters, all the parameters are in international units, and P in $\mu\text{C cm}^{-2}$. Furthermore, the temperature dependence of the lattice polarization is well fitted below T_C by

$$P \propto \sqrt{T_0 - T}. \quad (7)$$

Thus there are two main contributions in AS polarization, the lattice part and the part due to distortion of all the ions. Comparison of both contributions shows that they are of opposite signs (Fig. 10). Therefore the temperature dependence of the lattice polarization part can explain well the peculiar behavior of AS polarization, with a change of sign near 85 K. Moreover, owing to the inaccuracy of x-ray diffraction data on the position of hydrogen atoms, the results obtained in the framework of the point-charge model by Kwon and Kim¹⁷ are solely qualitative, viz., they only allow one to obtain the sign of the polarization due to distortion of the tetrahedral ions. For this reason, it is interesting to estimate the ionic distortion polarization part by the difference between the experimental polarization measured by Unruh⁵ and the lattice polarization (Fig. 10). The distortion part of the polarization appears suddenly at T_C and slightly decreases on cooling. This sudden appearance of the ionic polarization is, of course, due to the tetrahedral ordering.

Summarizing, at the phase transition, the loss of symmetry elements (ab mirror plane, center of inversion) and the increase of permanent dipoles induces a polarization due essentially to the distortion. Then on cooling the decrease of polarization is in the main due to the growth of the lattice contribution, and the change of sign at $\sim 85 \text{ K}$ corresponds simply to the fact that the lattice part of the polarization becomes larger than the distortion part.

C. Ammonium ν_3 internal-mode behavior

In the polarization $E \parallel a$, the internal ν_3 mode of NH_4^+ near 3000 cm^{-1} partially softens at a temperature T_1 , about 10 K above the phase-transition temperature T_C characterized by the discontinuity of sulfate modes previously discussed. The squared frequency of the $\text{NH}_4^+ \nu_3$ mode is linear with temperature below and above T_1 , with a ratio of slopes equal to 2 (Fig. 11). Another consequence of the first-order character of the phase transition

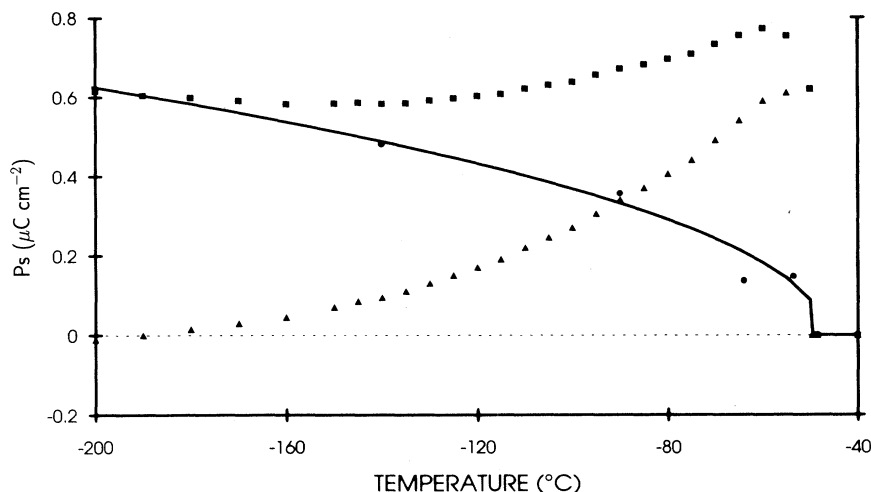


FIG. 10. Temperature dependence of spontaneous polarization of AS. Experimental values (Ref. 5) (triangles), contribution of the lattice polarization (circles) with its best fit (see text, full line), and the part due to the distortion of all the ions (squares).

is the discontinuity appearing at T_1 . Note that the oscillator strength of this mode is somewhat constant through the phase transition.

Such behavior is well explained in the framework of hard-mode spectroscopy, recently reviewed by Salje.²⁶ The phonon frequencies well above those of the soft mode depend on the variations of the structural order parameter as a function of temperature. The relative changes of phonon frequencies, usually below 2%, allow the treatment of the coupling between phonon frequencies ω and the order parameter Q in perturbation theory

$$\Delta(\omega^2) = A Q^m + B Q^{2m} . \quad (8)$$

The exponent $m = 1$ or 2 is determined by symmetry considerations ($m = 1$ is essentially the case of no symmetry breaking). For modes which are optically active above T_C one generally finds A far greater than B . Moreover,

for modes of such high frequency, the correlation length of hard modes is often comparable with the bond lengths so that the order parameter is measured on an atomistic length scale. This property allows the quantitative investigation of short-range order.

In the present case, the selection rules and the linear dependence of $\Delta(\omega^2)$ lead, respectively, to $m = 2$ and $A \gg B$. So the squared order parameter at an atomistic length scale is linear with T . The phase-transition temperature T_1 for the hard mode does not coincide with the temperature of the ferroelectric phase transition. Such behavior, also observed in $\text{Pb}_3(\text{PO}_4)_2$ for example,²⁶ is assigned to an intermediate regime (which is not a "phase" in the thermodynamic sense) characterized by strong short-range order and long-lived fluctuations of low-symmetry phase clusters. The short-range order of the intermediate regime is indistinguishable from long-range order in hard-mode spectroscopy so that the signatures of

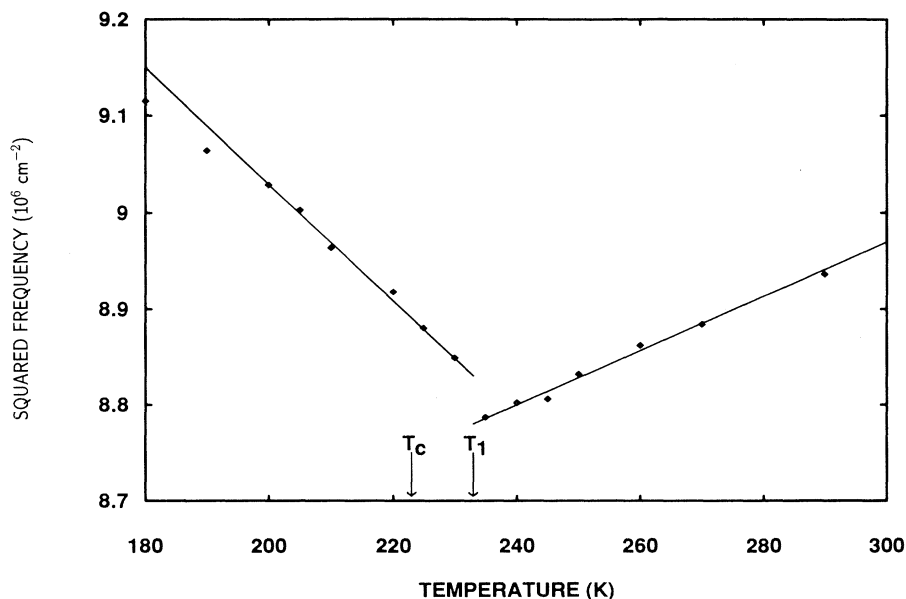


FIG. 11. Temperature dependence of the squared frequency of the internal ν_3 ammonium mode located at about 3000 cm^{-1} . The straight lines are obtained by least-squares fit. The ratio of slopes is equal to 2.

the low-symmetry configuration are established at $T_1 > T_C$.

VI. CONCLUSION

From investigation of infrared internal-mode reflectivity spectra, and comparison between AS and K_2SO_4 external modes associated with earlier ir, Raman, and structural data, the following conclusions can be drawn.

(i) No indication of softening was detected in the frequency range of sulfate internal modes for the B_{1u} and B_{3u} polarizations. The absence of softening of the ν_3 or ν_4 sulfate modes rules out the model of molecular distortion type.

(ii) Spectroscopic and structural signatures of the phase transition can be explained by a coupling with only one

order parameter Q of B_{1u} symmetry. The microscopic origin of the critical relaxation is tentatively attributed to the reorientation of the whole group $\text{NH}_4^+(\text{I})-(\text{SO}_4^{2-})-\text{NH}_4^+(\text{II})$ between two equivalent positions with regard to the ab mirror plane. This attribution is consistent with previous vibrational and structural studies.

(iii) The peculiar temperature dependence of the polarization is well explained by the present model with two contributions (lattice and distortion) of opposite signs, while the ferroelectric model, although it explains the behavior of the polarization, leads to too large values of the permanent dipoles.

ACKNOWLEDGMENTS

Fruitful discussions with Dr. F. Gervais and Pr. Y. Luspin are gratefully acknowledged.

-
- ¹B. T. Matthias and J. P. Remeika, *Phys. Rev.* **103**, 262 (1956).
²S. Hoshino, K. Vedam, Y. Okaya, and R. Pepinsky, *Phys. Rev.* **112**, 405 (1958).
³S. Ahmed, A. M. Shamah, R. Kamel, and Y. Badr, *Phys. Status Solidi A* **99**, 131 (1987).
⁴A. Onodera, O. Cynshi, and Y. Shiozaki, *J. Phys. C* **18**, 2831 (1984).
⁵H.-G. Unruh, *Solid State Commun.* **8**, 1951 (1970).
⁶A. Sawada, S. Ohya, Y. Ishibashi, and Y. Takagi, *J. Phys. Soc. Jpn.* **38**, 1408 (1975).
⁷E. O. Schlemper and W. C. Hamilton, *J. Chem. Phys.* **44**, 4498 (1966).
⁸G. V. Kozlov, S. P. Lebedev, A. A. Volkov, J. Petzelt, B. Wynncke, and F. Bréhat, *J. Phys. C* **21**, 4883 (1988).
⁹G. Luther and H.-G. Unruh, *Phys. Status Solidi A* **56**, 597 (1979).
¹⁰D. E. O'Reilly and T. Tsang, *J. Chem. Phys.* **46**, 1291 (1967).
¹¹N. Shibata, R. Abe, and I. Suzuki, *J. Phys. Soc. Jpn.* **41**, 2011 (1976).
¹²K. Hasebe and S. Tanisaki, *J. Phys. Soc. Jpn.* **42**, 568 (1977).
¹³K. Hasebe, *J. Phys. Soc. Jpn.* **50**, 1266 (1981).
¹⁴Z. Iqbal and C. W. Christoe, *Solid State Commun.* **18**, 269 (1976).
¹⁵H.-G. Unruh, E. Sailer, H. Hussinger, and O. Ayere, *Solid State Commun.* **25**, 871 (1978).
¹⁶H.-G. Unruh, J. Krüger, and E. Sailer, *Ferroelectrics* **20**, 3 (1978).
¹⁷S. B. Kwon and J. J. Kim, *J. Phys. Condens. Matter* **2**, 10607 (1990).
¹⁸T. Ikeda, K. Fujibayashi, T. Nagai, and J. Kobayashi, *Phys. Status Solidi A* **16**, 279 (1973).
¹⁹Y. S. Jain, P. K. Bajpai, R. Bhattacharjee, and D. Chowdhury, *J. Phys. C* **19**, 3789 (1986).
²⁰P. K. Bajpai and Y. S. Jain, *J. Phys. C* **20**, 387 (1987).
²¹D. W. Kydon, M. Pintar, and H. E. Petch, *J. Chem. Phys.* **47**, 1185 (1967).
²²T. J. Nordland, D. E. O'Reilly, and E. M. Peterson, *J. Chem. Phys.* **64**, 1838 (1976).
²³P. S. Goyal and B. A. Dasannacharya, *J. Chem. Phys.* **68**, 2430 (1978).
²⁴P. S. Goyal, R. Chakravarthy, B. A. Dasannacharya, and C. J. Carlile, *Phys. Status Solidi A* **118**, 425 (1990).
²⁵Sook-Il Kwun, Soon Gul Lee, Sang Youl Kim, and Jong-Gul Yoon, *Jpn. J. Appl. Phys.* **24**, Suppl. 24.2, 528 (1985).
²⁶E. K. H. Salje, *Phase Transitions* **37**, 83 (1992).
²⁷T. Kurosawa, *J. Phys. Soc. Jpn.* **16**, 1298 (1963).
²⁸F. Gervais, in *Infrared and Millimeter Waves*, edited by K. J. Button (Academic, New York, 1983), Vol. 8, Chap. 7, p. 279.
²⁹F. Bréhat and B. Wynncke, *J. Phys. C* **18**, 1705 (1985).
³⁰B. Wynncke and F. Bréhat, *Ferroelectrics* **80**, 861 (1988).
³¹K. Aizu, *J. Phys. Soc. Jpn.* **37**, 885 (1974).
³²Y. S. Jain and H. D. Bist, *Solid State Commun.* **15**, 1229 (1974).
³³A. Sawada, S. Ohya, Y. Ishibashi, and T. Takagi, *J. Phys. Soc. Jpn.* **38**, 1408 (1975).
³⁴A. Onodera, H. Fujishita, and Y. Shiozaki, *Solid State Commun.* **27**, 463 (1978).
³⁵A. Onodera, Y. Sugata, and Y. Shiozaki, *Solid State Commun.* **27**, 243 (1978).